Received: 3 November 2019 | Revised: 30 June 2020 | Accepted: 27 July 2020

DOI: 10.1111/gcb.15332

PRIMARY RESEARCH ARTICLE

Global Change Biology WILEY

A Bornean peat swamp forest is a net source of carbon dioxide to the atmosphere

Angela C. I. Tang[1,2] | Lulie Melling[1] | Paul C. Stoy[2,3] | Kevin K. Musin[1] | Edward B. Aeries[1] | Joseph W. Waili[1] | Mariko Shimizu[4] | Benjamin Poulter[5] | Ryuichi Hirata[6]

[1]Sarawak Tropical Peat Research Institute, Kota Samarahan, Sarawak, Malaysia

[2]Department of Land Resources and Environmental Sciences, Montana State University, Bozeman, MT, USA

[3]Department of Biological Systems Engineering, University of Wisconsin–Madison, Madison, WI, USA

[4]Civil Engineering Research Institute for Cold Region, Sapporo, Japan

[5]Biospheric Sciences Laboratory, NASA Goddard Space Flight Center, Greenbelt, MD, USA

[6]Center for Global Environmental Research, National Institute for Environmental Studies, Tsukuba, Japan

Correspondence
Lulie Melling, Sarawak Tropical Peat Research Institute, Kota Samarahan, Sarawak, Malaysia.
Email: luliemelling@gmail.com

Funding information
Sarawak State Government; National Science Foundation Department of Environmental Biology, Grant/Award Number: 1552976; Federal Government of Malaysia

[Correction added on 16 October 2020, after first online publication: minor changes have been made on pages 1 and 2 and 10 and 11 to improve readability.]

Abstract

Tropical peat forests are a globally important reservoir of carbon, but little is known about CO_2 exchange on an annual basis. We measured CO_2 exchange between the atmosphere and tropical peat swamp forest in Sarawak, Malaysia using the eddy covariance technique over 4 years from 2011 to 2014. The CO_2 fluxes varied between seasons and years. A small carbon uptake took place during the rainy season at the beginning of 2011, while a substantial net efflux of >600 g C/m^2 occurred over a 2 month period in the middle of the dry season. Conversely, the peat ecosystem was a source of carbon during both the dry and rainy seasons in subsequent years and more carbon was lost during the rainy season relative to the dry season. Our results demonstrate that the forest was a net source of CO_2 to the atmosphere during every year of measurement with annual efflux ranging from 183 to 632 g C m^{-2} year^{-1}, noting that annual flux values were sensitive to gap filling methodology. This is in contrast to the typical view of tropical peat forests which must have acted as net C sinks over time scales of centuries to millennia to create the peat deposits. Path analyses revealed that the gross primary productivity (GPP) and ecosystem respiration (RE) were primarily affected by vapour pressure deficit (VPD). Results suggest that future increases in VPD could further reduce the C sink strength and result in additional net CO_2 losses from this tropical peat swamp forest in the absence of plant acclimation to such changes in atmospheric dryness.

KEYWORDS

Borneo, carbon flux, CO_2 balance, eddy covariance, net ecosystem exchange, Southeast Asia, tropical peat swamp forest

1 | INTRODUCTION

With recent findings of peatlands in Amazon and Congo basins (Dargie et al., 2017; Draper et al., 2014), known tropical peatlands are distributed over 1.7 Mkm^2 (Gumbricht et al., 2017) and comprise 40% of the global peatland area (Xu, Morris, Liu, & Holden, 2018). The new discoveries reveal that the carbon pool of tropical peatland is four- to fivefold higher (Gumbricht et al., 2017) than the previous estimates (Maltby & Immirzi, 1993). While covering for only some 15% of the total area of tropical peatlands, Southeast Asian peatlands are a critical carbon reservoir with their extensive and thick deposits of peat. There remain considerable uncertainties about their present role in global carbon cycle. Tropical forests are now thought to represent a global net

Angela C. I. Tang and Lulie Melling should be considered joint first author.

C source (Baccini et al., 2017; Mitchard, 2018) but the role of tropical peat ecosystems to the carbon cycle remain unclear.

Previous studies in Southeast Asian peat forests have quantified soil CO_2 flux rates (Inubushi, Furukawa, Hadi, Purnomo, & Tsuruta, 2003; Jauhiainen, Takahashi, Heikkinen, Martikainen, & Vasander, 2005; Melling, Hatano, & Goh, 2005) with estimated emissions on the order of 950–2,100 g C m^{-2} $year^{-1}$. Higher emissions are intermittently observed during the dry season (Jauhiainen et al., 2005) but other studies find no distinct seasonal variability in soil CO_2 efflux (Inubushi et al., 2003; Melling et al., 2005). The role of seasonality in determining the net ecosystem CO_2 exchange (NEE) and gross primary productivity (GPP) of tropical peat ecosystems still needs to be ascertained. Because of the remoteness of locations and difficulty of measurements, there are to our knowledge only six tropical peatland sites with published NEE measurements. Among these six sites, three sites were located in Central Kalimantan, Indonesian Borneo (Palangkaraya, hereafter 'CK') with altered hydrology including clearcutting (Hirano et al., 2012), one was of a secondary forest in Sarawak, Malaysian Borneo (hereafter 'SF'; Kiew et al., 2018), and the other two were in primary and secondary forest in Thailand that employed a concentration gradient approach for CO_2 flux measurement (Suzuki, Ishida, Nagano, & Waijaroen, 1999). From these observations, the NEE in tropical peatlands was found to vary substantially at seasonal and interannual time scales, suggesting a high sensitivity to climate variability. The 4 year mean annual NEE for a relatively intact peat forest with minimal drainage in CK—including two El Niño years—was 174 ± 203 g C m^{-2} $year^{-1}$, varying year-to-year from a carbon sink (−27 g C m^{-2} $year^{-1}$) to a carbon source (443 g C m^{-2} $year^{-1}$; Hirano et al., 2012). Three years of NEE measurements at a peat forest disturbed by drainage exhibited higher seasonal variation such that the forest was a small CO_2 sink or approximately C neutral in the early dry season and emitted most CO_2 in the late dry season and/or early rainy season (Hirano et al., 2007). In contrast, a large amount of C was accumulated over 1 year in both primary (−532 g C m^{-2} $year^{-1}$) and secondary peat swamp forest (−522 g C m^{-2} $year^{-1}$) in Thailand (Suzuki et al., 1999) estimated using gradient techniques. The primary forest absorbed more carbon in the dry season than the rainy season, whereas the opposite was held for the secondary forest (Suzuki et al., 1999).

The role of a tropical peat forest as a net sink or source of CO_2 often depends on its response to climate and disturbance. Hirano et al. (2012) found that the CO_2 balance of three peat ecosystems in CK was principally controlled by groundwater level (GWL), in which the NEE increased (i.e. the ecosystems became a stronger C source or weaker C sink) when GWL decreased on an annual basis, and suggested that a lowering of 0.1 m of GWL increased the CO_2 efflux rates by 79–238 g C m^{-2} $year^{-1}$. Carbon uptake at the CK sites was also constrained by decreases in photosynthetic photon flux density (PPFD) caused by atmospheric ozone production from nearby peat fires and high values of the vapour pressure deficit (VPD), consistent with findings that plant stomata respond to VPD values greater than c. 1 kPa (Fu et al., 2019; Körner, 1995; Oren et al., 1999). The seasonal effects on carbon cycling were also observed in South America's tropical ecosystems, where water availability via rainfall imposes a major ecophysiological constraint on photosynthesis or/and respiration (Goulden et al., 2004; Malhi et al., 1998; Vourlitis et al., 2001) such that the annual C balance is particularly sensitive to climate anomalies (Cavaleri et al., 2017; Hutyra et al., 2007).

The interannual variability of NEE in undrained tropical peat forests has not been measured to date. A functional and mechanistic understanding of the response of ecosystem-scale CO_2 flux to hydrological and meteorological changes will improve models used to estimate the regional and global C budgets and to predict ecosystem responses to global climate change. Such results can also contribute to global CO_2 mitigation efforts. The aim of this paper is to improve the state of current knowledge of tropical peat forests with respect to the seasonal and interannual variability in NEE and its components, GPP and ecosystem respiration (RE) and the role played by environmental factors including changes in atmospheric radiation and ozone that may result from peat fires elsewhere in Southeast Asia in controlling CO_2 exchange.

2 | MATERIALS AND METHODS

2.1 | Site description

The study was carried out in tropical peat swamp forest in Maludam National Park in the Betong Division of Sarawak, Malaysia. Maludam National Park is situated on the Maludam Peninsula between the Saribas River to the north and the Lupar River to the south—both draining into South China Sea—and consists entirely of low-lying flat peat swamp with uneven microrelief and a hummocky surface (Melling & Hatano, 2004; Figure 1). The Park was officially gazetted in 2000 with an areal extent of 43,200 ha. It was further protected with an extension of 10,421 ha in 2015, making it the largest tract of protected peat swamp in Northern Borneo. The forests were selectively logged before it was declared a National Park in 2000. The peatland exhibits domed profiles. When the peat is saturated, excess water flows radially across the surface of the peat dome into the surrounding waterways. Such phenomenon divides the peat swamp into several catchments. Because of the low relief and interlinked catchments in the coastal lowlands, their boundaries are not fixed nor well defined (Kselik & Tie, 2004). Under natural condition, the catchment areas vary over time due to extreme weather (Kselik & Tie, 2004) or/and changes in the peat surface elevation (Melling & Hatano, 2004). The water table is close to or above the peat surface throughout the year and fluctuates with rainfall intensity and duration.

Peat in Sarawak is generally classified as the ombrogenous peat (rain fed) and therefore poor in nutrients (oligotrophic). Depending on the floristic composition and structure which are strongly affected by topographic and hydrologic gradients, six different forest types (or phasic communities, PC) generally occur in a concentric sequence on the peat dome in Sarawak (Anderson, 1963). These range

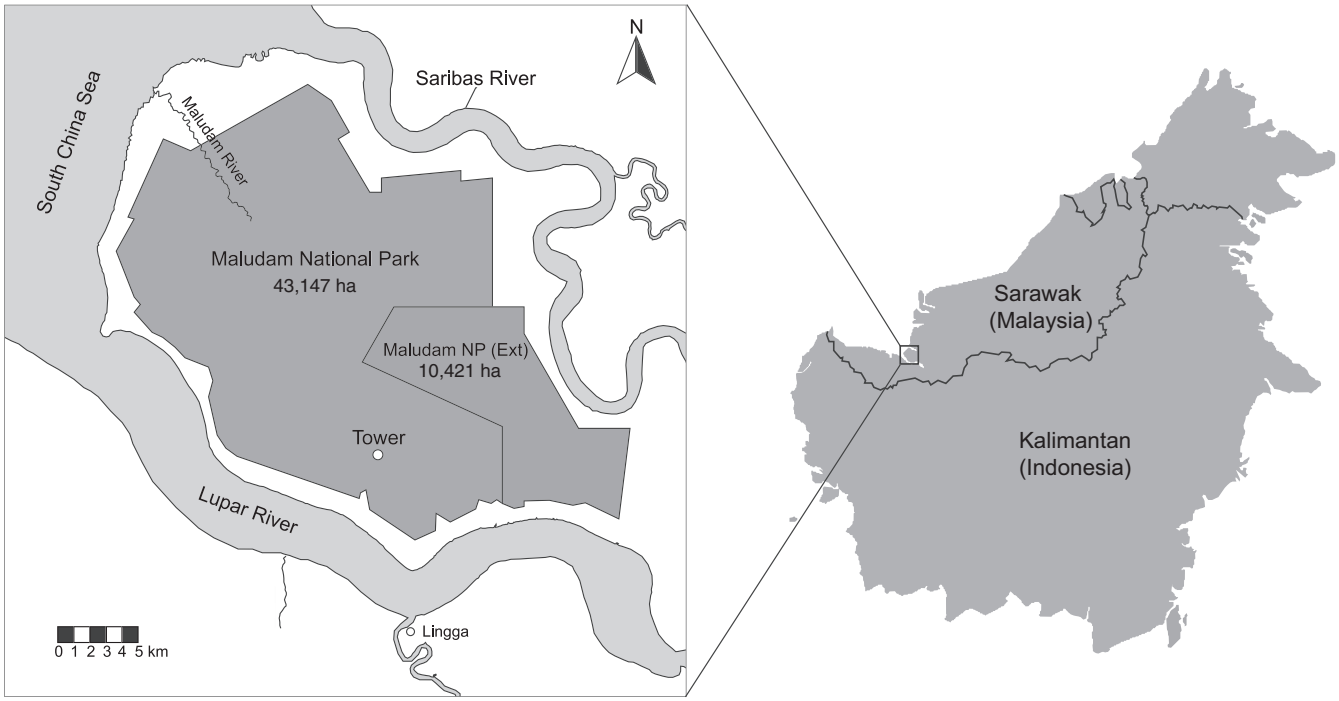

FIGURE 1 A map of the study site in Maludam National Park, Sarawak, Malaysian Borneo

from mixed swamp forest with structure and physiognomy similar to lowland dipterocarp rainforest on the more fertile periphery of the dome, to stunted with xeromorphic features in the centre of the dome with increasing peat thickness, acidity and lower fertility.

The flux tower was established in Alan Batu forest (PC2; 1°27′13″N, 111°8′58″E) which has an uneven and irregular canopy with an average height of 35 m. The Alan Batu forest is dominated by large, scattered trees of Alan (*Shorea albida*) with girth greater than 3.5 m. Most of these large trees have hollow stems and staghead crowns. This forest is found on the edge of the dome with abiotic stresses. Therefore, *S. albida* has adapted to develop large buttresses that are almost invariably hollow and extensive root systems which commonly creates vacant layers of about 20–30 cm within the top 100 cm of peat soil. Other dominant tree species include *Lithocarpus* sp., *Litsea* sp. and *Stemonurus* sp. while the lower canopy mainly consists of young trees, shrubs, ferns, sedges, pandanus and pitcher plants. The forest floor was covered with a layer of organic tree debris, consisting mainly of decaying tree leaves. Plant area index (PAI) was measured monthly from January 2014 to December 2014 using a LI-2200 plant canopy analyser (LI-COR Inc.). Average PAI was 6.2 m^2/m^2 with no significant seasonal changes in 2014 ($p = .674$). The terrain in the vicinity of the tower is relatively flat (slope < 2°) with an elevation of 8 m above mean sea level and peat thickness of c. 9 m.

2.2 | Measurements of fluxes and micrometeorological variables

NEE was measured continuously using the eddy covariance (EC) technique over 4 years from 2011 to 2014. The EC system was mounted at the tip of a long boom with an extension of 1 m from the 40 m tower and consisted of a LI-7500A open-path CO_2/H_2O analyser (LI-COR), which measured the concentrations of CO_2 and water vapour, coupled to a CSAT3 three-dimensional sonic anemometer (Campbell Scientific Inc.) facing the direction of the prevailing wind (southeast, Figure S1a), which measured the three components of wind velocity at 10 Hz that were logged using a CR3000 Datalogger (Campbell Scientific) as described in Tang et al., (2019). A LI-820 closed-path CO_2 analyser (LI-COR) was deployed to measure the vertical profile of CO_2 concentration at six levels within the canopy at 0.5, 1, 3, 11, 21 m and above the canopy at 41 m. Air was drawn from each inlet at the tower and the sampling path was rotated every minute. Thus, the measurement for six levels took 6 min and the concentration was averaged over 30 min.

Net radiation was measured at 41 m using a CNR4 net radiometer (Kipp & Zonen). Two LI-190SB quantum sensors (LI-COR) were likewise mounted at 41 m and pointed downwards and upwards to measure incoming and outgoing PPFD. Air temperature (T_{air}) and relative humidity were measured at 11 and 41 m using CS215 temperature and relative humidity probes (Campbell Scientific). The tower was also equipped with a three-cup anemometer and wind vane (01003-5, R.M. Young Co.) at 41 m to measure wind speeds and wind directions in addition to the sonic anemometer. Rainfall was measured by a TE525MM tipping-bucket rain gauge (Texas Electronics) 1 m above the ground surface in an open area located c. 5 m from the tower. Soil temperature was measured about 20 m from the tower with platinum resistance thermocouples at 5 cm below the ground surface. Volumetric soil water content was measured at a depth of 30 cm at two locations (flat area and hummocky terrain) using CS616 time domain reflectometry (Campbell Scientific). The readings from two locations were averaged

to represent the overall moisture of the measurement area. All meteorological variables were continuously recorded using CR3000 and CR1000 data loggers at a sampling frequency of 5 min and averaged over each 30 min period except GWL, which was monitored 20 m away from the tower on a half-hourly basis using a water level logger (DL/N 70 STS Sensor, Technik Sirnach AG).

2.3 | Data processing, gap filling and uncertainty analysis

Postprocessing calculations were performed using Flux Calculator (Ueyama et al., 2012), and included spike removal, double rotation (Wilczak, Oncley, & Stage, 2001), time-lag corrections, frequency response corrections (Massman, 2000, 2001) and density fluctuation corrections (Webb, Pearman, & Leuning, 1980) to calculate the EC flux, F_c.

NEE was calculated as the sum of F_c and the storage flux (F_s). The F_s was calculated using vertical CO_2 concentration (c) profiles (Aubinet et al., 2001):

$$F_s = \frac{P_a}{RT_a}\int_0^h \frac{\partial c(z)}{\partial t}dz, \quad (1)$$

where P_a, R and T_{air} are respectively the ambient pressure (N/m^2), molar constant (N m mol^{-1} K^{-1}) and air temperature (K), and h, $c(z)$, t and z represent the measurement height of F_c (m), the CO_2 mixing ratio (μmol/mol), time (s), and vertical distance from ground surface (m).

We used the atmospheric stability threshold (Novick et al., 2004), which requires near-neutral atmospheric stability for night-time (PPFD < 5 μmol m^{-2} s^{-1}) data acceptance. Atmospheric stability is defined as $\zeta = (z - d)/L$, where z is the measurement height of the sonic anemometer, d is the zero-plane displacement and L is the Obukhov length. An additional u^* threshold value of 0.1 m/s was included to ensure that observations with insufficient turbulence were excluded from the analysis, which is infrequently observed after applying the u^* filter. We tested the sensitivity of our results using a u^* threshold alone, which was calculated as 0.177, 0.191, 0.201 and 0.196 m/s for 2011, 2012, 2013 and 2014 respectively using Flux Analysis Tool software (Ueyama et al., 2012). In a similar study of CO_2 exchange, a u^* threshold value of 0.15 m/s was applied for the SF site that is located approximately 25 km from the studied site (Kiew et al., 2018) whereas 0.17 m/s threshold value was implemented for a case study for methane flux at the same site (Wong et al., 2018). Observations that exceeded logical upper bounds of 50 μmol m^{-2} s^{-1} and lower bounds of 50 μmol m^{-2} s^{-1} were also excluded from data records. Before quality control, the rate of missing due to power failure, instruments malfunction and program error was 31.3%. There was a continuous long gap of observations for about 50 days in 2011 from August 20 until October 10, and 46 days in 2014 from November 15 until December 31. After quality-filtering, 36% of NEE data remained between January 2011 and December 2014. Specifically, the data gaps are 64.1%, 62.1%, 61.9% and 62.4% for 2011, 2012, 2013 and 2014 respectively.

The use of night-time methods for gap filling these missing data struggled to adequately sample night-time RE as implemented in the REddyProc package and REddyProc online tool (Reichstein, Moffat, Wutzler, & Sickel, 2014) due in part to the intermittent nature of nocturnal turbulence in tropical forest canopies in which low-frequency perturbations impact canopy flows more readily than turbulence (e.g. Santos et al., 2016). Furthermore, the relatively low variability of air and soil temperatures across the year make it a challenge to model the response of RE to temperature. Using daytime-based methods avoids these problems. We chose the Mitscherlich model (Aubinet et al., 2001; Reichstein, Stoy, Desai, Lasslop, & Richardson, 2012) because of its improvement in estimating GPP at light saturation versus the rectangular hyperbola as discussed in Reichstein et al. (2012).

$$NEE = -(\beta_M + \gamma_M)\left(1 - \exp\left(\frac{-\alpha_M PPFD}{\beta_M + \gamma_M}\right)\right) + \gamma_M, \quad (2)$$

where α_M is the initial slope of the light response curve, β_M is the GPP at light saturation and γ_M is the intercept parameter at PPFD = 0 μmol m^{-2} s^{-1}, representing RE. Parameters were estimated using least squares regression for observations within a 7 day moving window of NEE and PPFD observations. Parameter sets during periods for which the parameter estimation routine did not converge to an optimal solution or for which observations were not available were estimated using the values from the preceding period. GPP was calculated as the difference between the estimated RE and the observed NEE: GPP = RE − NEE, thereby combining the meteorological convention that negative NEE indicates ecosystem CO_2 uptake and the physiological convention that GPP is positive. We also tested this approach against the Marginal Distribution Sampling approach for data gap filling in Table S1 and Figure S2 to provide a conservative estimate of net CO_2 fluxes given that annual flux values are subject to uncertainty due to calculation technique (Stoy et al., 2006).

We applied the paired daily-difference approach (Hollinger & Richardson, 2005; Richardson et al., 2006) to estimate the random uncertainty of NEE. Random uncertainty was quantified using measurement pairs that were selected if the mean half-hourly PPFD for two successive days differed by less than 75 μmol m^{-2} s^{-1}, air temperature differed by less than 3°C and wind speed differed by less than 1 m/s. Random uncertainty was then propagated through the gap filling routines by perturbing the input flux observations with a random value drawn from a normal distribution multiplied by the previously calculated random errors (Motulsky & Ransnas, 1987). This procedure was iterated for 100 times such that 100 gap filling models were fit for each day using least squares regressions. Missing NEE data were filled using the mean of the 100 models. Gap filling uncertainty was determined as the standard deviation of the annual sums. Total uncertainty for each annual period attributable to random uncertainty and gap filling uncertainty was calculated using the root-sum-square method. The uncertainty procedure is similar to that described in Vick, Stoy, Tang, and Gerken (2016). The mean annual uncertainty in NEE was 96.6 ± 3.4 g C m^{-2} year^{-1}, random

uncertainty of which dominates about 92%–97% of the total uncertainty for 2011–2014. A flux source area analysis is presented in Figure S1b.

2.4 | Path analysis

To understand the effects of environmental controls on ecosystem carbon exchange, we performed path analysis for monthly means of data using the lavaan' package in R (Rosseel, 2012). We first constructed two separate conceptual models assuming (a) GPP was mainly controlled by PPFD, VPD and volumetric water content (VWC) which were related to T_{air} (i.e. clear skies with more radiation increase T_{air} which is itself used in the VPD calculation) and rainfall; and (b) RE was mainly controlled by GWL and VPD that were associated with T_{air}, VWC and rainfall. The final path diagrams were derived after adding or removing paths based on the overall fit of the path analysis model that was assessed using χ^2 test ($p > .05$), root mean square error of approximation (RMSEA < 0.08) and comparative fit index (CFI > 0.95; Schreiber, Nora, Stage, Barlow, & King, 2006).

2.5 | Inferred variables

We estimated the diffuse radiation fraction (K_d) using the clearness index (K_t)—the ratio of global solar radiation (R_g) to the extra-terrestrial solar radiation (R_o; Spitters, Toussaint, & Goudriaan, 1986)—related to atmospheric transmissivity. This approach provides the basis for models that perform well in K_d model intercomparisons (Oliphant & Stoy, 2018). We also used the tropospheric ozone product from the NASA Global Modelling Initiative that was calculated on an hourly basis by combining inference from remote sensing and a three-dimensional (3-D) chemistry and transport model as described by Wargan et al. (2017). We use these data products to explore the sensitivity of carbon fluxes of the tropical peat swamp forest to variability in diffuse radiation and atmospheric ozone concentrations.

3 | RESULTS

3.1 | Seasonal and annual patterns in climatic variables

The annual pattern of rainfall in Sarawak is characterized by a dry season, which typically lasts from April to September, and a rainy season, which typically lasts from October to March. We used the median (246 mm) as the threshold to separate the dry and rainy periods for the 16 year rainfall collected at Lingga meteorological station. Thus, the dry season for 16 year rainfall was determined for April to September with average monthly rainfall less than 246 mm, whereas the rainy season from October to March with rainfall greater than 246 mm, noting that the southwest monsoon generally occurs from May to September, and the northeast monsoon from November to March. Annual rainfall during the study period was 3,289, 3,072, 2,691 and 2,091 mm in 2011, 2012, 2013 and 2014, respectively (Figure 2a; Table 1). Rainfall during the October–March rainy season accounted for 69%, 74%, 59% and 54% of the annual sum, respectively, during 2011, 2012, 2013 and 2014. The annual cumulative PPFD was 4.7% greater in 2013 (6,152 MJ m^{-2} $year^{-1}$) than in 2011 (5,877 MJ m^{-2} $year^{-1}$), whereas comparable cumulative PPFD was observed in 2012 and 2014 (6,015 and 6,017 MJ m^{-2} $year^{-1}$, respectively; Figure 2b; Table 1). T_{air} increased sequentially over the 4 year study period with annual means of 26.6, 26.9, 27 and 27.1°C in 2011, 2012, 2013 and 2014, respectively (Figure 2c; Table 1). May was the warmest month during 2011 and 2012, whereas the maximum monthly T_{air} was recorded during June in 2013 and July in 2014. The average daytime VPD increased by 0.19, 0.27, 0.18 and 0.18 kPa, respectively during the dry seasons of 2011, 2012, 2013 and 2014 compared with the rainy season (Figure 2d; Table 1). The monthly average of daytime VPD reached a maximum of 0.85, 0.98, 0.89 and 0.99 kPa respectively in July 2011, June 2012, June 2013 and July 2014. The observed soil moisture (Figure 2e) exhibited substantial seasonal and interannual variations during the entire study period and GWL frequently shifted from positive values (i.e. standing water) to negative values (Figure 2f).

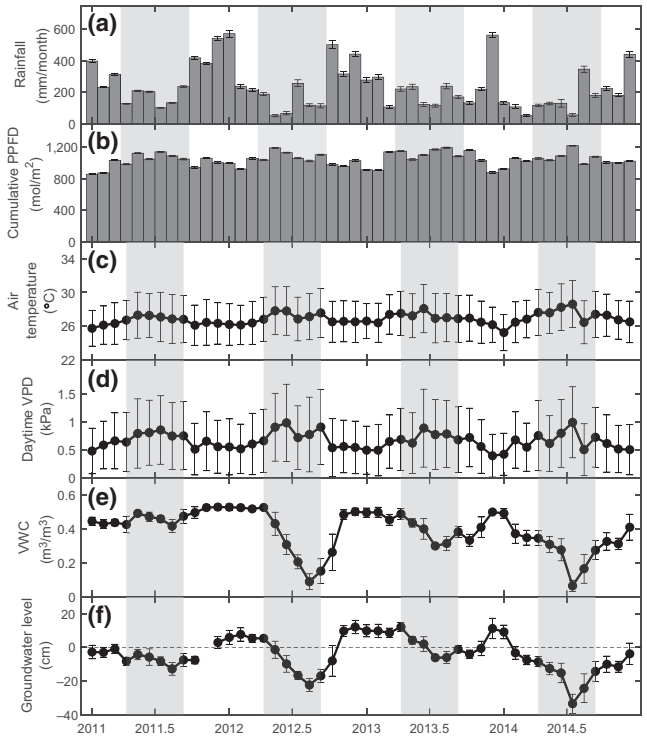

FIGURE 2 Seasonal variations in monthly sums of (a) rainfall and (b) photosynthetic photon flux density (PPFD), and monthly means of (c) air temperature (T_{air}), (d) daytime vapour pressure deficit (VPD), (e) volumetric water content (VWC) and (f) groundwater level (GWL) during the study period from 2011 to 2014. Vertical bars denote one standard deviation. The shaded areas represent the dry seasons

TABLE 1 Annual sums of net ecosystem exchange of CO_2 (NEE), ecosystem respiration (RE), gross primary productivity (GPP), rainfall, photosynthetic photon flux density (PPFD) and annual mean of air temperature, daytime vapour pressure deficit (VPD), volumetric soil water content and groundwater level with standard deviation from 2011 to 2014 at a tropical peat swamp forest in Sarawak, Malaysian Borneo. Mean ± standard deviation over four study years are given in lowermost line

Year	NEE (g C m^{-2} $year^{-1}$)	RE (g C m^{-2} $year^{-1}$)	GPP (g C m^{-2} $year^{-1}$)	Rainfall (mm)	Cumulative PPFD (kmol m^{-2} $year^{-1}$)	Air temperature (°C)	Daytime VPD[a] (kPa)	Volumetric soil water content (m^3/m^3)	Groundwater level (cm)
2011	632 ± 93	2,563 ± 247	1,931 ± 285	3,289 ± 55	12.2 ± 0.03	26.6 ± 2.6	0.67 ± 0.54	0.47 ± 0.05	−5.3 ± 5.2
2012	509 ± 96	2,782 ± 104	2,273 ± 246	3,072 ± 55	12.5 ± 0.02	26.9 ± 2.7	0.69 ± 0.58	0.38 ± 0.17	−2.5 ± 12.2
2013	183 ± 101	2,637 ± 154	2,454 ± 288	2,691 ± 47	12.8 ± 0.03	27.0 ± 2.6	0.65 ± 0.55	0.42 ± 0.08	3.2 ± 7.4
2014	356 ± 97	3,199 ± 106	2,843 ± 302	2,091 ± 48	12.5 ± 0.03	27.1 ± 2.6	0.64 ± 0.53	0.31 ± 0.12	−11.3 ± 11.4
Mean ± *SD*	420 ± 194	2,795 ± 284	2,375 ± 380	2,786 ± 525	12.5 ± 0.5	26.9 ± 0.2	0.66 ± 0.02	0.39 ± 0.07	−4.0 ± 6.0

[a]Daytime VPD was averaged at PPFD greater than 5 μmol m^{-2} s^{-1}.

3.2 | Seasonal and annual surface-atmosphere CO_2 exchange

The annual course of cumulative NEE (Figure 3a) exhibited different responses to climatic and hydrologic variability during the 4 year observation period. In 2011, approximately 76 g C/m^2 was taken up during the rainy season in the early portion of the calendar year and the early dry season before mid-June. In other words, the forest was a net carbon sink from January until the middle of the dry season in mid-June, after which increasing RE (Figure 3b) and declining GPP (Figure 3c) resulted in a large carbon loss event of >600 g/m^2 over a 2 month period (Figure 3a). GPP then increased from 50 g C m^{-2} $month^{-1}$ in August to 222 g C m^{-2} $month^{-1}$ in September

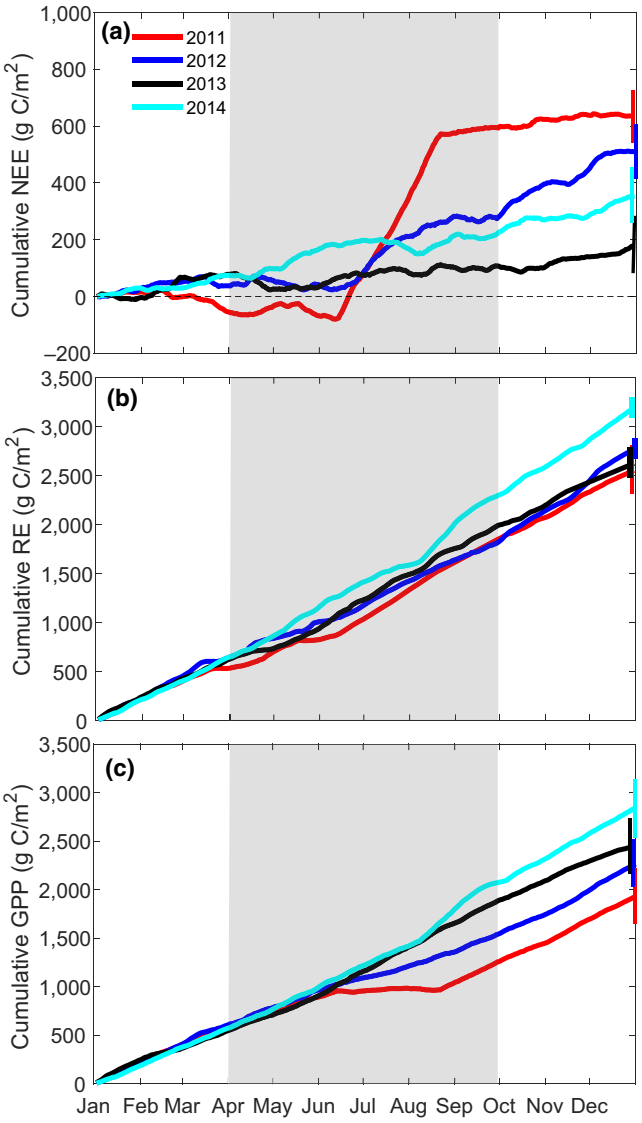

FIGURE 3 The cumulative sum of (a) net ecosystem CO_2 exchange (NEE), (b) ecosystem respiration (RE) and (c) gross primary productivity (GPP) at a tropical peat swamp forest site in Maludam National Park, Sarawak, Malaysian Borneo for 2011, 2012, 2013 and 2014. Error bars represent the uncertainty estimate. The shaded area represents the dry season

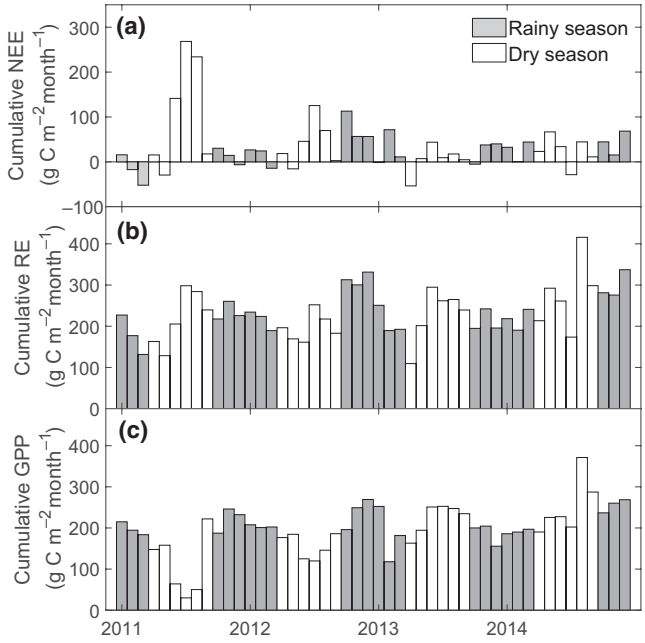

FIGURE 4 Monthly time series of cumulative (a) net ecosystem CO_2 exchange (NEE), (b) ecosystem respiration (RE) and (c) gross primary production (GPP) at a tropical peat swamp forest site in Maludam National Park, Sarawak, Malaysian Borneo from 2011 to 2014. Uncertainties about annual sums are presented in Figure 3

2011 (Figure 4), almost enough to offset the respiration rates, leading to a small carbon source for the month. Despite the relatively large C sink during the first part of 2011, the forest exhibited the largest C source during the second part of the year such that measured NEE during 2011 was 632 ± 93 g C m^{-2} year^{-1}, that is, a net C source to the atmosphere. Random uncertainty contributed more than 90% and gap filling uncertainty less than 10% of the total annual NEE uncertainty estimates.

GPP averaged 198 g C m^{-2} month^{-1} during the rainy season and the early dry season of 2012, but began to decline in the middle of dry season to 125 g C m^{-2} month^{-1}, and the forest lost 241 g C/m^2 to the atmosphere in June, July and August 2012. The seasonal trends of NEE in 2011 and 2012 were similar, except for the last quarter of 2012, where RE increased by 36% versus 2011, which resulted in large carbon loss despite an increased GPP during the October–December rainy season. Measured NEE during 2012 was 509 ± 96 g C m^{-2} year^{-1}.

Contrary to 2011 and 2012, ecosystem carbon uptake in 2013 increased during the middle of the dry season, totalling 751 g C/m^2 from June to August, whereas only 144 g C/m^2 and 391 g C/m^2 accumulated during this period in 2011 and 2012 respectively. Consequently, the forest released less carbon during the dry season in 2013. A small sink of 29 g C/m^2 was observed in July of 2014; NEE in 2014 had a similar seasonal pattern but was less variable than during 2013.

Annual RE was not statistically significantly different from 2011 to 2013 (p = .720) and took values of 2,563 ± 247, 2,782 ± 104 and 2,637 ± 154 g C m^{-2} year^{-1}, respectively (Table 1). Annual RE increased in 2014 to 3,199 ± 106 g C m^{-2} year^{-1}, concomitant with an increase in annual GPP (Figure 3b,c; Table 1). In 2012, RE was significantly greater during the rainy season than during the dry season (p = .029), but no statistically significant difference was found between rainy and dry seasons during 2011, 2013 and 2014.

Annual GPP increased from year to year and took values of 1,931 ± 285, 2,273 ± 246, 2,454 ± 288 and 2,843 ± 302 g C m^{-2} year^{-1} for 2011, 2012, 2013 and 2014, respectively (Table 1). Monthly averaged GPP was lower during the dry season than the rainy season in both 2011 (p = .014) and 2012 (p = .004), but the opposite was held for the following 2 years. Dry season GPP accounted for 35%, 41%, 55% and 53% of annual GPP for 2011–2014, respectively. The maximum canopy photosynthesis rate (β) was lowest in 2011 (30.5 μmol m^{-2} s^{-1}; Figure 5a) and dry season β was lower during 2011 (20.6 μmol m^{-2} s^{-1}) and 2012 (21.2 μmol m^{-2} s^{-1}) than 2013 (33.7 μmol m^{-2} s^{-1}) and 2014 (33.6 μmol m^{-2} s^{-1}; Figure 5b). GPP occurred at similar rates during the early part of each year but differed during the dry season among years (Figures 3 and 4c). GPP took its highest monthly value during the rainy season in 2011 (November) and 2012 (December), but during the dry season in 2013 (July) and 2014 (August). Minimum monthly GPP was observed during the middle of the dry season in July during 2011 and 2012, but during

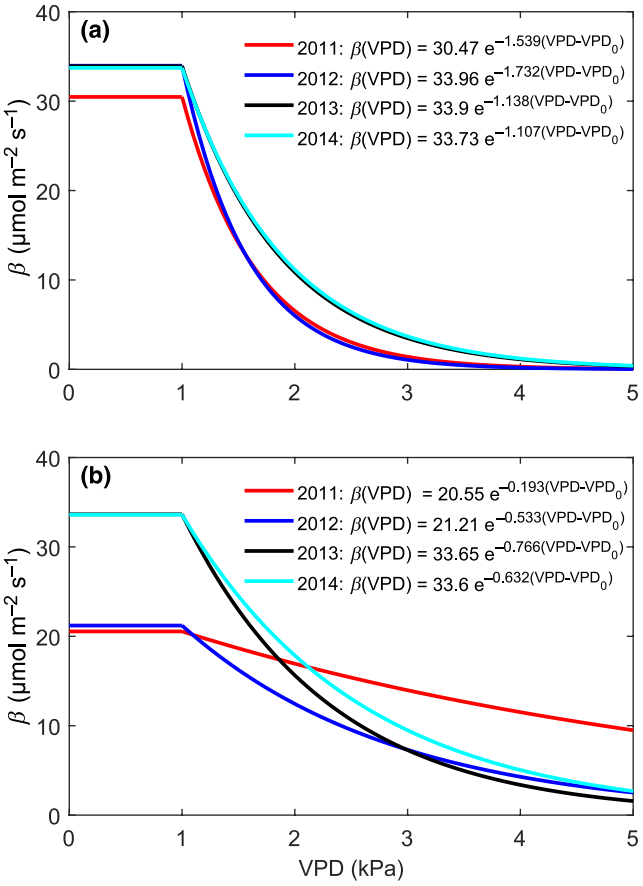

FIGURE 5 The function decreasing the maximum CO_2 uptake parameter β_M as a function of VPD following the formulation of Lasslop et al. (2010) during DOY (a) 1–365 and (b) 165–234 corresponding to the dry season

the rainy season in February and January during 2013 and 2014 respectively.

3.3 | Effects of VPD on GPP and NEE

GPP was limited by higher VPD (greater than ~1 kPa), which caused an increase in NEE (indicating less ecosystem CO_2 uptake, Figure 6), as also revealed by the path analysis (Figure S3a). NEE tended to increase (become less negative) under high VPD conditions regardless of PPFD (Figure 7). In 2011, under high atmospheric dryness with VPD greater than 1 kPa, NEE decreased linearly (i.e. ecosystem carbon uptake increased) as PPFD increased, until approximately 1,100 μmol m^{-2} s^{-1}, at which NEE started to increase from −5.5 μmol m^{-2} s^{-1} to −2.9 μmol m^{-2} s^{-1} at a PPFD of 1,580 μmol m^{-2} s^{-1}. A similar but smaller effect on NEE was also observed in 2012 when VPD was greater than 1 kPa. A mean positive slope of 0.0025 was observed for the NEE–VPD relationship at high PPFD of 1,100–1,800 μmol m^{-2} s^{-1} during 2011, but the slope was negative, as −0.0049, −0.008 and −0.0051 for 2012, 2013 and 2014, respectively.

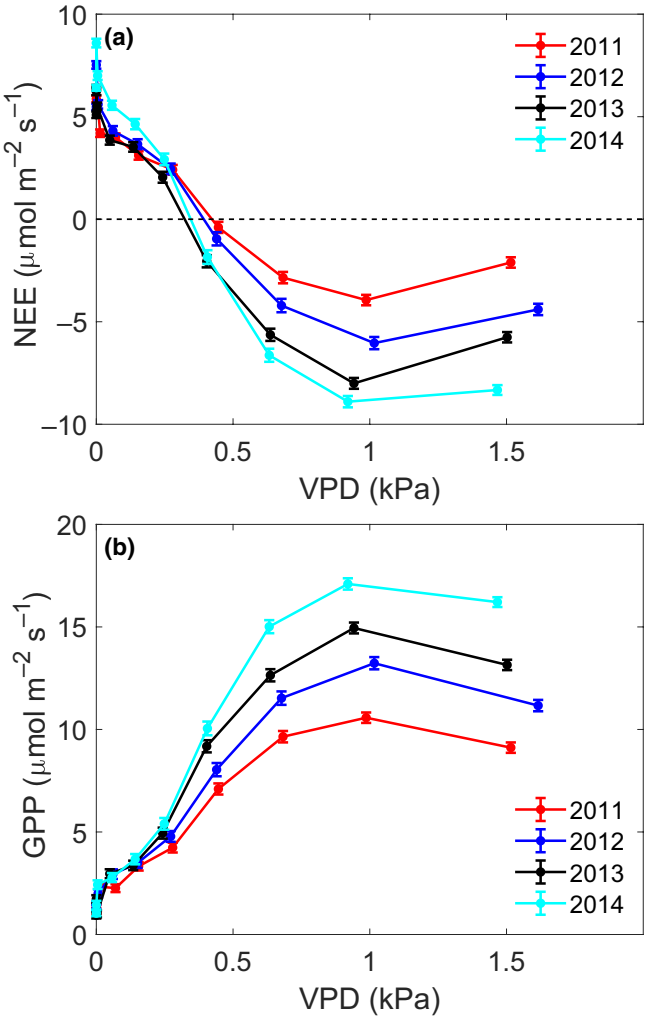

FIGURE 6 Effects of vapour pressure deficit (VPD) on (a) net ecosystem exchange (NEE) and (b) GPP for 2011–2014. Half-hourly NEE and GPP were sorted into deciles based on VPD. Each point represents the average of half-hourly NEE and GPP for each decile

3.4 | Clearness index and diffuse radiation fraction

Using daytime data between 10 and 14 hr LST, the 3 month (June–August) average clearness index (K_t) are not significantly different between measurement years ($p = .475$). The diffuse fraction (K_d) was lowest in 2013 (0.462), followed by 2014 (0.504), 2012 (0.509) and 2011 (0.520). On an average annual basis, K_t in 2011 was lowest in 2011 (0.505), which resulted in the highest K_d (0.593) among measurement years (Figure S4).

The relationship between GPP, NEE with K_d was nearly constant at low K_d. GPP and NEE only became sensitive to change in K_d at high levels of K_d for 2012, 2013 and 2014 (Figure S5). In 2011, however, we observed an initial rapid increase in GPP and decrease in NEE with K_d but began to decline (increase) after the maximum at a diffuse fraction of 0.65.

3.5 | Ozone

We investigated the potential effects of ozone on CO_2 fluxes during the measurement period (Figure S6). There were no significant seasonal differences in ozone (O_3) concentration between measurement years (paired t test, $p > .05$). However, the O_3 concentration was generally slightly higher during the dry season (~23 ppb) than during the rainy season (~21 ppb) of 2011, 2012 and 2014.

4 | DISCUSSION

We focus our discussion on the mechanisms that underlie the unique features of the RE and GPP time series and their implications for NEE including the observation that monthly RE was higher in the rainy season of 2012 than other years, that monthly averaged GPP was higher in the rainy season than the dry season in both 2011 and 2012 but not subsequent years, and the large net CO_2 loss observed during the dry season of 2011 (Figures 3 and 4; Table 1).

4.1 | Ecosystem respiration

Annual sums of RE were not significantly different between 2011, 2012 and 2013, but were higher in 2014 (Table 1) in parallel with the highest T_{air} and GPP, and lowest GWL and soil moisture observed during the measurement period. RE increased as the dry seasons of 2011, 2013 and 2014 progressed (Figure 4b) and decreased during the rainy season. These observations are consistent with the notion that inadequate oxygen supplies in saturated conditions restrict aerobic decomposition of organic matter in tropical soils (Chambers et al., 2004), and the lowering of the water table enhances microbial

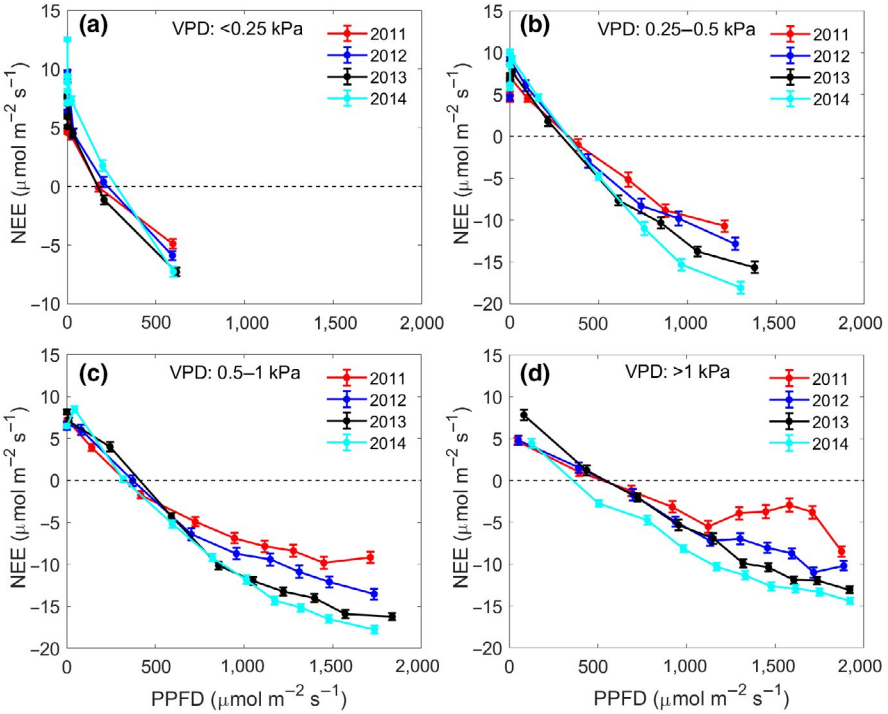

FIGURE 7 Effects of photosynthetic photon flux density (PPFD) on net ecosystem exchange (NEE) at different levels of vapour pressure deficit (VPD) at (a) <0.25 kPa, (b) 0.25–0.5 kPa, (c) 0.5–1 kPa and (d) >1 kPa, for 2011–2014. Half-hourly NEE were sorted into deciles based on the PPFD. Each point represents the average of half-hourly NEE for each decile

decomposition (Figure 2f). In 2012, however, the site received 26% of annual rainfall when it comprised 31%, 41% and 46% of the 2011, 2013 and 2014 annual rainfall, respectively, during the dry season. GWL declined to 17–22 cm below the ground surface alongside low soil moisture content (0.09–0.2 m^3/m^3) in 2012 as a consequence. The unique hydrological conditions observed resulted in a pulse increase in RE following rewetting; over the next 3 months (October–December) of rainy season conditions, respiration was stimulated (Figure 4) following the increases in rainfall inputs and soil moisture content despite a small decrease in temperature (Figure 2c). The rewetting of dry soil induced a flush of respiration during this period and thus the average respiration rate in the rainy season was 2.3 g C m^{-2} day^{-1} greater than that of the dry season in 2012. Likewise, the pulse following increased rainfall by 291 mm increased the respiration by 242 g C/m^2 in August 2014 (Figures 2a and 4b).

The rewetting effect, consistent with the Birch effect (Jarvis et al., 2007), was observed at the same study site that the soil CO_2 fluxes measured using an automated chamber system were found after the rapid rise in GWL from −4 cm to 19 cm over 4 days in November 2015 (Ishikura et al., 2019). Lower GWL enhances soil aeration, which promotes oxidative peat decomposition and gas diffusion in the soil. The high CO_2 flux due to rewetting effect might result from the following phenomena as discussed in Ishikura et al. (2019): (a) soil microbes that are killed during GWL drawdown are easily decomposed during subsequent rewetting (Fraser et al., 2016; Marumoto, Kai, Yoshida, & Harada, 1977), (b) soil microbial activity is enhanced by the rewetting despite the unchanging population size (Fraser et al., 2016; Placella, Brodie, & Firestone, 2012) and (c) the rise in GWL and soil moisture can physically displace CO_2 that are accumulated in soil air during the dry period (Huxman et al., 2004). The rewetting effect can last for from a few hours to a few weeks (Borken & Matzner, 2009; Bowling, Grote, & Belnap, 2011). A similar observation was found at an old-growth tropical forest in Brazil (Goulden et al., 2004), where the rapid increase in RE following increased rainfall released microbes from water stress within the litter layer after dry season desiccation..

Otherwise, monthly averaged RE was similar but slightly greater during dry seasons (0.37–0.58 g C m^{-2} day^{-1}) and coincided with a small increase in T_{air} (Figure 2c). In other words, the seasonal variation in RE was related to T_{air} as well as water supply when reduced rainfall caused GWL drawdown and a decline in soil moisture with a stimulation of RE following the very dry 2012 dry season. Relationships between RE and GPP were less clear, in part due to the strong suppression of GPP observed during the 2011 dry season.

4.2 | Gross primary productivity

GPP was reduced by VPD values above ~1 kPa during all measurement years (Figure 6b), consistent with leaf and ecosystem-level syntheses (Körner, 1995; Lasslop et al., 2010; Oren et al., 1999; Reichstein et al., 2012) as well as recent studies of tropical forest ecosystems (Fu et al., 2018; Kiew et al., 2018; Wu et al., 2017). However, our findings are consistent with a decrease in GPP with VPD ~1 kPa, Fu et al. (2018) found that GPP was sensitive to VPD at values lower than 1 kPa across tropical forests. The decay rate parameter *k* (Lasslop et al., 2010) was lowest (i.e. GPP was less sensitive to VPD) during the dry season of 2011, followed by 2012, 2014 and 2013 (Figure 5b), consistent with the notion that stomatal sensitivity to VPD increases as a function of canopy conductance in the absence of VPD limitations (Oren et al., 1999). When all days of each year were included, the photosynthetic rate declined fastest with

VPD at 1.73 kPa in 2012, followed by 2011 at 1.54 kPa, suggesting seasonal variability in the sensitivity of GPP to VPD needs to be explored further using species-level observations of plant hydraulics. Based on these results, we infer that the decrease in GPP during June–August of 2011 and 2012 as well as the seasonal variation in GPP for these 2 years was affected by VPD and of course PPFD (Figure 7) rather than differences in diffuse radiation fraction (K_d; Figure S4b), ozone (Figure S6) or GWL given that GWL was lowest during the 2014 dry season (Figure 2f) when GPP was at its highest on a monthly basis (Figure 4c). What is less clear for the case of the present study is why GPP in 2011 was more sensitive to VPD at high levels of PPFD (Figure 7d), especially during periods when K_d was low (Fig. S4b), which resulted in the strong suppression of GPP during the 2011 dry season.

The 2011 dry season reduction in GPP might in part attributed to the relative clearness indices (K_t) and resulting K_d (Figure 4; Figures S4 and S5; Knohl & Baldocchi, 2008). Hirano et al. (2012) also found that smoke in an El Niño year reduced annual net CO_2 uptake by 17% at a relatively intact peat forest with little drainage in Indonesia. Low K_t at the study site is largely due to aerosols from massive fires, largely in Indonesia, that occur during fire season from early June to late October (Yulianti & Hayasaka, 2013). Total PPFD, however, was not anomalously low during the 2011 dry season (Figure 2b), and increases in diffuse radiation tend to increase canopy photosynthesis due to enhanced canopy radiation penetration if PPFD itself is not decreased (Gu et al., 2003). Changes in total or diffuse PPFD are therefore unlikely to have caused low GPP during the 2011 dry season, which largely occurred under conditions of direct radiation. As noted above, ozone concentrations are not estimated to have been anomalously high during the 2011 dry season (Figure S6).

Tropical forests may reduce canopy conductance more strongly to increase VPD than other terrestrial ecosystems because they are often more isohydric than other ecosystems (Fisher, Williams, Do Vale, Da Costa, & Meir, 2006). But tropical trees exist along the isohydric to anisohydric hydraulic continuum (Klein, 2014) and anisohydricity may be preferred in tropical systems with low risk of water stress (Kumagai & Porporato, 2012). The area surrounding the flux tower may be dominated by species or individuals that may reside in different spots along the isohydricity continuum and the spatial variability of isohydricity should be explored across global ecosystems, but the wind rose analysis does not suggest that the flux source area was different during the 2011 dry season which excludes a source area explanation for the 2011 anomaly (Figure S1b).

The annual GPP, unlike RE, increased between all measurement years and took the values 1,931 ± 285, 2,273 ± 246, 2,454 ± 288 and 2,843 ± 302 g C m^{-2} $year^{-1}$, for 2011, 2012, 2013 and 2014, respectively ($p < .01$; Table 1). While the lowest VPD was observed in 2014, we found that the forest productivity was more affected by atmospheric dryness than soil water stress, noting that the site received the least rainfall concomitant with lowest soil moisture and GWL in 2014 among all measurement years (Table 1). A similar result was described by Sulman et al. (2016) who found that VPD fluctuations accounted for significant reductions of GPP regardless of changes in soil moisture content in a temperate hardwood forest. Several studies also highlight the increasing importance of atmospheric constraint for ecosystem fluxes as the rising VPD under warming climate could limit stomatal conductance and evapotranspiration and thus reduce ecosystem CO_2 uptake (Novick et al., 2016; Sulman et al., 2016). Pau, Detto, Kim, and Still (2018), and on the other hand, demonstrated that GPP was more strongly correlated with radiometric canopy temperature (T_{can}) than T_{air} or VPD in which the GPP increased with warming T_{can} but declined at T_{can} above 31–32°C during the afternoon in line with long-term observations (Sullivan et al., 2020). Therefore, a warming climate may reduce tropical forest productivity as T_{can} may reach a temperature threshold earlier in the day unless plants are able to acclimate to this temperature stress. We tested the impacts of radiometric surface temperature (T_{surf}) on GPP in Figure S7. T_{surf}, dominated by canopy temperature (T_{can}) varied little across the measurement years ($p > .05$). The rate of photosynthesis in 2011 was relatively low with rising temperature and declined faster at high temperature threshold (Figure S7). From these results, the decline in photosynthesis at the study site appears to be driven by high VPD and temperature (Figure 6; Figure S7), noting that Pau et al. (2018) deployed thermal cameras and were able to explore differences in stem and canopy temperatures, whereas our radiometric observations integrate these over the field of view of the radiometer. From these observations, we cannot exclude the notion that the large 2011 CO_2 loss may be due to lagged response to anomalously warm years and also disturbances that may have occurred before the observation period as has been found in other tropical rainforests (Hayek et al., 2018; Saleska et al., 2003) including the 2010 dipterocarp masting event. We also note the impacts of the strong El Niño event of 2015–16 on NEE in a tropical rainforest in central Sulawesi, Indonesia (Gushchina et al., 2019); the magnitude of NEE decreased because of the strong RE increase and muted GPP increase to the warmer and sunnier conditions, emphasizing the importance of long-term flux records for understanding ecosystem response to the full range of potential climate conditions.

4.3 | Comparison with other tropical forests

The annual NEE of 420 ± 194 g C m^{-2} $year^{-1}$ for this study site, resulting from a balance between RE of 2,795 ± 284 g C m^{-2} $year^{-1}$ and GPP of 2,375 ± 380 g C m^{-2} $year^{-1}$, is higher than that of two other Bornean peat swamp forests (Hirano et al., 2012; Kiew et al., 2018). In Palangkaraya, Central Kalimantan of Indonesia, a relatively undrained peat swamp forest (CK) was a small carbon sink (−27 g C m^{-2} $year^{-1}$) or carbon source (72 g C m^{-2} $year^{-1}$) during La Niña years but turned into a large source of 20–443 g C m^{-2} $year^{-1}$ in El Niño years due to declining GWL or/and dense smoke from peat fires (Hirano et al., 2012). Similarly, the drought associated with El Niño events switched the Amazonian forests from carbon sink to carbon source of about 100 g C m^{-2} $year^{-1}$, with decomposition of coarse woody debris making a major contribution to carbon loss (Hutyra et al., 2007; Saleska et al., 2003). In contrast, a

secondary peat swamp forest (SF), located c. 25 km from the study site took up 98–207 g C m^{-2} $year^{-1}$ over the same measurement period (Kiew et al., 2018). The difference can be attributed in part to the higher PAI (7.9 m^2/m^2) and lower GWL (−19 cm) at the SF. A net carbon sink of >100 C m^{-2} $year^{-1}$ has also been identified in several Amazonian and Asian rainforests (Fu et al., 2018; Goulden et al., 2004; Kosugi et al., 2008; Loescher, Oberbauer, Gholz, & Clark, 2003).

The RE and GPP at the study site are low relative to two Bornean peat swamp forests (RE: 3,642 g C m^{-2} $year^{-1}$, GPP: 3,468 g C m^{-2} $year^{-1}$, Hirano et al., 2012; RE: 3,546 g C m^{-2} $year^{-1}$, GPP: 3,682 g C m^{-2} $year^{-1}$, Kiew et al., 2018). GWL at these sites is on average 49 cm (CK) and 15 cm (SF) lower than that of our study site. In addition to the lower PAI (5 m^2/m^2), the CK site was also drier with average annual rainfall of 2,452 mm and daytime VPD that was often more than twice that of our study site (Hirano et al., 2012). Using automated chamber systems, the annual soil CO_2 emission was less at our study site (Ishikura et al., 2019) than the CK site (Sundari, Hirano, Yamada, Kusin, & Limin, 2012) by 421 g C m^{-2} $year^{-1}$. These results further imply that small decreases in GWL in tropical peatlands need not reduce water availability for the biochemical and physiological processes of trees, but rather enhance soil aeration, which leads to an increase in substrate availability and gas diffusion rates. Such hydrologic controls on microbial communities have been observed in tropical and boreal peatlands, of which oxygen constraints represent a pivotal factor on decomposition (Freeman, Ostle, Fenner, & Kang, 2004; Kwon, Haraguchi, & Kang, 2013). Increasing substrate supply from photosynthesis under low GWL condition also tends to increase leaf and below-ground respiration (Hartley et al., 2006). On the other hand, soil inundation depletes soil oxygen, which in turn, adversely affects plant growth by altering metabolic processes. The early decline in the photosynthesis rate of flooded plants typically is associated with stomatal closure (Kozlowski, 1982; Pezeshki, 1993) and prolonged flooding impedes photosynthetic capacity which may involve changes in carboxylation enzymes, loss of chlorophyll and reduced leaf area because of inhibition of leaf formation and expansion as well as leaf abscission (Kozlowski & Pallardy, 1997).

In addition to vertical eddy fluxes, we cannot exclude methane flux and lateral carbon export through discharge—including carbon import to the flux footprint and subsequent outgassing—for a full ecosystem carbon balance. The methane contribution is, however, negligible to the overall carbon balance of the tropical peat forest; the study area was a net source of C-CH_4 on the order of 10 g C m^{-2} $year^{-1}$ (Tang et al., 2018; Wong et al., 2018). Müller et al. (2015) estimated a dissolved organic carbon flux of 63 g C m^{-2} $year^{-1}$ from the Maludam catchment located c. 12–25 km from the tower site which accounts for more than 99% of the total organic carbon. When we include methane and fluvial carbon loss terms in carbon balance, the total carbon lost from the tropical peat forest in our study increases by 17% before accounting for other minor fluxes including volatile organic compound and animal-associated C transport which were not measured in the present study.

5 | CONCLUSION

Nearly all studied peat forests in Borneo observed to date were net losses of CO_2 to the atmosphere on an annual basis, on average, regardless of large-scale climate oscillations and meteorological variability. This is in contrast to the typical behaviour of tropical rainforests, which are often CO_2 sinks but have the potential to turn into CO_2 sources under drought stress (Fu et al., 2018). Given that substantial peat deposits at peat forest study sites indicate long-term carbon uptake on the time scales of soil development, it is unclear if multiyear net carbon losses to the atmosphere or low carbon sink capacity are a feature of peat forests, or if recent changes in ecosystem behaviour—perhaps in response to climate variability—have tipped these ecosystems to be net annual carbon sources over the long term. The latter seems more plausible as the peat forests must have acted as net C sinks over time scales of centuries to millennia to create the peat deposits while several studies corroborate that the unexpected strong carbon releases were driven by warmer temperature as a consequence of declines in primary productivity (Arnone et al., 2008; Ciais et al., 2005; Hayek et al., 2018) and increased heterotrophic respiration (Arnone et al., 2008). Therefore, we cannot rule out the large carbon source observed in 2011 might be the lagged effects of warming climate which reverse centuries of carbon sequestration; we note that the measurement years were more than 0.6°C warmer than the 1985–2015 average and more than 1°C warmer than the mid-1980s based on the CRU database (Figure S8a), noting that the study ecosystem was transitioning from a period of relatively wet years from 2008 to 2010 to a drier period during 2014 and 2015. Longer term records are necessary to investigate the decadal responses of tropical peat forests to forest demography and climate variability. Future studies should seek to address the paradoxical result that tropical peat forests measurements indicate substantial CO_2 sources to the atmosphere on an annual basis, an 'emergent C source' across tropical forests that may already be happening (Mitchard, 2018)and understand any potential acclimation of tropical tree species to ongoing increases in T_{air} and VPD (Fu et al., 2018; Novick et al., 2016).

ACKNOWLEDGEMENTS

This work was supported by the Sarawak State Government and the Federal Government of Malaysia. P.C.S. acknowledges support from the National Science Foundation Department of Environmental Biology grant #1552976. We thank the Department of Irrigation and Drainage, Sarawak for sharing rainfall data. We are grateful to Takashi Hirano for his advice and assistance in this study, Rob Payn, Mark Greenwood, Tobias Gerken, William Kleindl, Gabriel Bromley, Adam Cook, Mallory Morgan, and Amy Trowbridge for their valuable feedback on an earlier version of the manuscript. We also thank the Subject Editor and three anonymous reviewers for their constructive comments that helped us to improve the clarity and scientific rigor of this manuscript.

CONFLICT OF INTEREST

We declare no conflict of interest.

DATA AVAILABILITY STATEMENT

The data that support the findings of this study are available from the corresponding author upon reasonable request.

ORCID

Angela C. I. Tang https://orcid.org/0000-0002-8733-6484
Lulie Melling https://orcid.org/0000-0003-4480-517X
Benjamin Poulter https://orcid.org/0000-0002-9493-8600

REFERENCES

Anderson, J. A. R. (1963). The flora of the peat swamp forests of Sarawak and Brunei, including a catalogue of all recorded species of flowering plants, ferns and fern allies. *Gardens' Bulletin Singapore*, *20*, 131–228.

Arnone III, J. A., Verburg, P. S., Johnson, D. W., Larsen, J. D., Jasoni, R. L., Lucchesi, A. J., … Schimel, D. S. (2008). Prolonged suppression of ecosystem carbon dioxide uptake after an anomalously warm year. *Nature*, *455*(7211), 383–386. https://doi.org/10.1038/nature07296

Aubinet, M., Chermanne, B., Vandenhaute, M., Longdoz, B., Yernaux, M., & Laitat, E. (2001). Long term carbon dioxide exchange above a mixed forest in the Belgian Ardennes. *Agricultural and Forest Meteorology*, *108*(4), 293–315. https://doi.org/10.1016/S0168-1923(01)00244-1

Baccini, A., Walker, W., Carvalho, L., Farina, M., Sulla-Menashe, D., & Houghton, R. A. (2017). Tropical forests are a net carbon source based on aboveground measurements of gain and loss. *Science*, *358*(6360), 230–234. https://doi.org/10.1126/science.aam5962

Borken, W., & Matzner, E. (2009). Reappraisal of drying and wetting effects on C and N mineralization and fluxes in soils. *Global Change Biology*, *15*(4), 808–824. https://doi.org/10.1111/j.1365-2486.2008.01681.x

Bowling, D. R., Grote, E. E., & Belnap, J. (2011). Rain pulse response of soil CO_2 exchange by biological soil crusts and grasslands of the semi-arid Colorado Plateau, United States. *Journal of Geophysical Research: Biogeosciences*, *116*(G3). https://doi.org/10.1029/2011JG001643

Cavaleri, M. A., Coble, A. P., Ryan, M. G., Bauerle, W. L., Loescher, H. W., & Oberbauer, S. F. (2017). Tropical rainforest carbon sink declines during El Niño as a result of reduced photosynthesis and increased respiration rates. *New Phytologist*, *216*(1), 136–149. https://doi.org/10.1111/nph.14724

Chambers, J. Q., Tribuzy, E. S., Toledo, L. C., Crispim, B. F., Higuchi, N., Santos, J. D., … Trumbore, S. E. (2004). Respiration from a tropical forest ecosystem: Partitioning of sources and low carbon use efficiency. *Ecological Applications*, *14*(sp4), 72–88. https://doi.org/10.1890/01-6012

Ciais, P. H., Reichstein, M., Viovy, N., Granier, A., Ogée, J., Allard, V., … Valentini, R. (2005). Europe-wide reduction in primary productivity caused by the heat and drought in 2003. *Nature*, *437*(7058), 529–533. https://doi.org/10.1038/nature03972

Dargie, G. C., Lewis, S. L., Lawson, I. T., Mitchard, E. T., Page, S. E., Bocko, Y. E., & Ifo, S. A. (2017). Age, extent and carbon storage of the central Congo Basin peatland complex. *Nature*, *542*(7639), 86–90. https://doi.org/10.1038/nature21048

Draper, F. C., Roucoux, K. H., Lawson, I. T., Mitchard, E. T., Coronado, E. N. H., Lähteenoja, O., … Baker, T. R. (2014). The distribution and amount of carbon in the largest peatland complex in Amazonia. *Environmental Research Letters*, *9*(12), 124017. https://doi.org/10.1088/1748-9326/9/12/124017

Fisher, R. A., Williams, M., Do Vale, R. L., Da Costa, A. L., & Meir, P. (2006). Evidence from Amazonian forests is consistent with isohydric control of leaf water potential. *Plant, Cell & Environment*, *29*(2), 151–165. https://doi.org/10.1111/j.1365-3040.2005.01407.x

Fraser, F. C., Corstanje, R., Deeks, L. K., Harris, J. A., Pawlett, M., Todman, L. C., … Ritz, K. (2016). On the origin of carbon dioxide released from rewetted soils. *Soil Biology and Biochemistry*, *101*, 1–5. https://doi.org/10.1016/j.soilbio.2016.06.032

Freeman, C., Ostle, N. J., Fenner, N., & Kang, H. (2004). A regulatory role for phenol oxidase during decomposition in peatlands. *Soil Biology and Biochemistry*, *36*(10), 1663–1667. https://doi.org/10.1016/j.soilbio.2004.07.012

Fu, Z., Gerken, T., Bromley, G., Araújo, A., Bonal, D., Burban, B., … Stoy, P. C. (2018). The surface-atmosphere exchange of carbon dioxide in tropical rainforests: Sensitivity to environmental drivers and flux measurement methodology. *Agricultural and Forest Meteorology*, *263*, 292–307. https://doi.org/10.1016/j.agrformet.2018.09.001

Fu, Z., Stoy, P. C., Poulter, B., Gerken, T., Zhang, Z., Wakbulcho, G., & Niu, S. (2019). Maximum carbon uptake rate dominates the interannual variability of global net ecosystem exchange. *Global Change Biology*, *25*(10), 3381–3394. https://doi.org/10.1111/gcb.14731

Goulden, M. L., Miller, S. D., Da Rocha, H. R., Menton, M. C., de Freitas, H. C., Figueira, A. M. E. S., & de Sousa, C. A. D. (2004). Diel and seasonal patterns of tropical forest CO_2 exchange. *Ecological Applications*, *14*(sp4), 42–54. https://doi.org/10.1890/02-6008

Gu, L., Baldocchi, D. D., Wofsy, S. C., Munger, J. W., Michalsky, J. J., Urbanski, S. P., & Boden, T. A. (2003). Response of a deciduous forest to the Mount Pinatubo eruption: Enhanced photosynthesis. *Science*, *299*(5615), 2035–2038. https://doi.org/10.1126/science.1078366

Gumbricht, T., Roman-Cuesta, R. M., Verchot, L., Herold, M., Wittmann, F., Householder, E., … Murdiyarso, D. (2017). An expert system model for mapping tropical wetlands and peatlands reveals South America as the largest contributor. *Global Change Biology*, *23*(9), 3581–3599. https://doi.org/10.1111/gcb.13689

Gushchina, D., Heimsch, F., Osipov, A., June, T., Rauf, A., Kreilein, H., … Knohl, A. (2019). Effects of the 2015–2016 El Niño event on energy and CO_2 fluxes of a tropical rainforest in Central Sulawesi, Indonesia. *Geography, Environment, Sustainability*, *12*(2), 183–196. https://doi.org/10.24057/2071-9388-2018-88

Hartley, I. P., Armstrong, A. F., Murthy, R., Barron-Gafford, G., Ineson, P., & Atkin, O. K. (2006). The dependence of respiration on photosynthetic substrate supply and temperature: Integrating leaf, soil and ecosystem measurements. *Global Change Biology*, *12*(10), 1954–1968. https://doi.org/10.1111/j.1365-2486.2006.01214.x

Hayek, M. N., Longo, M., Wu, J., Smith, M. N., Restrepo-Coupe, N., Tapajós, R., … Wofsy, S. C. (2018). Carbon exchange in an Amazon forest: From hours to years. *Biogeosciences*, *15*(15), 4833–4848. https://doi.org/10.5194/bg-15-4833-2018

Hirano, T., Segah, H., Harada, T., Limin, S., June, T., Hirata, R., & Osaki, M. (2007). Carbon dioxide balance of a tropical peat swamp forest in Kalimantan, Indonesia. *Global Change Biology*, *13*(2), 412–425. https://doi.org/10.1111/j.1365-2486.2006.01301.x

Hirano, T., Segah, H., Kusin, K., Limin, S., Takahashi, H., & Osaki, M. (2012). Effects of disturbances on the carbon balance of tropical peat swamp forests. *Global Change Biology*, *18*(11), 3410–3422. https://doi.org/10.1111/j.1365-2486.2012.02793.x

Hollinger, D. Y., & Richardson, A. D. (2005). Uncertainty in eddy covariance measurements and its application to physiological models. *Tree Physiology*, *25*(7), 873–885. https://doi.org/10.1093/treephys/25.7.873

Hutyra, L. R., Munger, J. W., Saleska, S. R., Gottlieb, E., Daube, B. C., Dunn, A. L., … Wofsy, S. C. (2007). Seasonal controls on the exchange of carbon and water in an Amazonian rain forest. *Journal of Geophysical Research: Biogeosciences*, *112*(G3). https://doi.org/10.1029/2006JG000365

Huxman, T. E., Snyder, K. A., Tissue, D., Leffler, A. J., Ogle, K., Pockman, W. T., … Schwinning, S. (2004). Precipitation pulses and carbon fluxes in semiarid and arid ecosystems. *Oecologia*, *141*(2), 254–268. https://doi.org/10.1007/s00442-004-1682-4

Inubushi, K., Furukawa, Y., Hadi, A., Purnomo, E., & Tsuruta, H. (2003). Seasonal changes of CO_2, CH_4 and N_2O fluxes in relation to land-use change in tropical peatlands located in coastal area of South Kalimantan. *Chemosphere*, *52*(3), 603–608. https://doi.org/10.1016/S0045-6535(03)00242-X

Ishikura, K., Hirata, R., Hirano, T., Okimoto, Y., Wong, G. X., Melling, L., … Ishii, Y. (2019). Carbon dioxide and methane emissions from peat soil in an undrained tropical peat swamp forest. *Ecosystems*, *22*(8), 1852–1868. https://doi.org/10.1007/s10021-019-00376-8

Jarvis, P., Rey, A., Petsikos, C., Wingate, L., Rayment, M., Pereira, J., … Valentini, R. (2007). Drying and wetting of Mediterranean soils stimulates decomposition and carbon dioxide emission: The "Birch effect". *Tree Physiology*, *27*(7), 929–940. https://doi.org/10.1093/treephys/27.7.929

Jauhiainen, J., Takahashi, H., Heikkinen, J. E., Martikainen, P. J., & Vasander, H. (2005). Carbon fluxes from a tropical peat swamp forest floor. *Global Change Biology*, *11*(10), 1788–1797. https://doi.org/10.1111/j.1365-2486.2005.001031.x

Kiew, F., Hirata, R., Hirano, T., Wong, G. X., Aeries, E. B., Musin, K. K., … Melling, L. (2018). CO_2 balance of a secondary tropical peat swamp forest in Sarawak, Malaysia. *Agricultural and Forest Meteorology*, *248*, 494–501. https://doi.org/10.1016/j.agrformet.2017.10.022

Klein, T. (2014). The variability of stomatal sensitivity to leaf water potential across tree species indicates a continuum between isohydric and anisohydric behaviours. *Functional Ecology*, *28*(6), 1313–1320. https://doi.org/10.1111/1365-2435.12289

Knohl, A., & Baldocchi, D. D. (2008). Effects of diffuse radiation on canopy gas exchange processes in a forest ecosystem. *Journal of Geophysical Research: Biogeosciences*, *113*(G2). https://doi.org/10.1029/2007JG000663

Körner, C. (1995). Leaf diffusive conductances in the major vegetation types of the globe. In E. D. S. & M. M. Caldwell (Eds.), *Ecophysiology of photosynthesis* (pp. 463–490). Springer. https://doi.org/10.1007/978-3-642-79354-7_22

Kosugi, Y., Takanashi, S., Ohkubo, S., Matsuo, N., Tani, M., Mitani, T., … Nik, A. R. (2008). CO_2 exchange of a tropical rainforest at Pasoh in Peninsular Malaysia. *Agricultural and Forest Meteorology*, *148*(3), 439–452. https://doi.org/10.1016/j.agrformet.2007.10.007

Kozlowski, T. T. (1982). Water supply and tree growth. Part II. Flooding. *Forestry Abstracts*, *43*(3), 145–161.

Kozlowski, T. T., & Pallardy, S. G. (1997). *Growth control of woody plants*. San Diego, CA: Academic Press.

Kselik, R. A. L., & Tie, Y. L. (2004). Hydrology of the peat swamp in the Maludam National Park Betong Division Sarawak. Tech. Rep., Alterra/Forest Department Sarawak/Sarawak Forestry Corporation, Kuching, Sarawak, Malaysia.

Kumagai, T. O., & Porporato, A. (2012). Strategies of a Bornean tropical rainforest water use as a function of rainfall regime: Isohydric or anisohydric? *Plant, Cell & Environment*, *35*(1), 61–71. https://doi.org/10.1111/j.1365-3040.2011.02428.x

Kwon, M. J., Haraguchi, A., & Kang, H. (2013). Long-term water regime differentiates changes in decomposition and microbial properties in tropical peat soils exposed to the short-term drought. *Soil Biology and Biochemistry*, *60*, 33–44. https://doi.org/10.1016/j.soilbio.2013.01.023

Lasslop, G., Reichstein, M., Papale, D., Richardson, A. D., Arneth, A., Barr, A., … Wohlfahrt, G. (2010). Separation of net ecosystem exchange into assimilation and respiration using a light response curve approach: Critical issues and global evaluation. *Global Change Biology*, *16*(1), 187–208. https://doi.org/10.1111/j.1365-2486.2009.02041.x

Loescher, H. W., Oberbauer, S. F., Gholz, H. L., & Clark, D. B. (2003). Environmental controls on net ecosystem-level carbon exchange and productivity in a Central American tropical wet forest. *Global Change Biology*, *9*(3), 396–412. https://doi.org/10.1046/j.1365-2486.2003.00599.x

Malhi, Y., Nobre, A. D., Grace, J., Kruijt, B., Pereira, M. G., Culf, A., & Scott, S. (1998). Carbon dioxide transfer over a Central Amazonian rain forest. *Journal of Geophysical Research: Atmospheres*, *103*(D24), 31593–31612. https://doi.org/10.1029/98JD02647

Maltby, E., & Immirzi, P. (1993). Carbon dynamics in peatlands and other wetland soils regional and global perspectives. *Chemosphere*, *27*(6), 999–1023. https://doi.org/10.1016/0045-6535(93)90065-D

Marumoto, T., Kai, H., Yoshida, T., & Harada, T. (1977). Drying effect on mineralizations of microbial cells and their cell walls in soil and contribution of microbial cell walls as a source of decomposable soil organic matter due to drying. *Soil Science and Plant Nutrition*, *23*(1), 9–19. https://doi.org/10.1080/00380768.1977.10433017

Massman, W. J. (2000). A simple method for estimating frequency response corrections for eddy covariance systems. *Agricultural and Forest Meteorology*, *104*(3), 185–198. https://doi.org/10.1016/S0168-1923(00)00164-7

Massman, W. J. (2001). Reply to comment by Rannik on "A simple method for estimating frequency response corrections for eddy covariance systems". *Agricultural and Forest Meteorology*, *107*(3), 247–251. https://doi.org/10.1016/S0168-1923(00)00237-9

Melling, L., & Hatano, R. (2004). Peat soils study of the peat swamp in the Maludam National Park Betong Division Sarawak. Tech. Rep., Alterra/Forest Department Sarawak/Sarawak Forestry Corporation. Kuching, Sarawak, Malaysia.

Melling, L., Hatano, R., & Goh, K. J. (2005). Soil CO_2 flux from three ecosystems in tropical peatland of Sarawak, Malaysia. *Tellus B: Chemical and Physical Meteorology*, *57*(1), 1–11. https://doi.org/10.3402/tellusb.v57i1.16772

Mitchard, E. T. (2018). The tropical forest carbon cycle and climate change. *Nature*, *559*(7715), 527–534. https://doi.org/10.1038/s41586-018-0300-2

Motulsky, H. J., & Ransnas, L. A. (1987). Fitting curves to data using nonlinear regression: A practical and nonmathematical review. *The FASEB Journal*, *1*(5), 365–374. https://doi.org/10.1096/fasebj.1.5.3315805

Müller, D., Warneke, T., Rixen, T., Müller, M., Jamahari, S., Denis, N., … Notholt, J. (2015). Lateral carbon fluxes and CO_2 outgassing from a tropical peat-draining river. *Biogeosciences*, *12*(20), 5967–5979. https://doi.org/10.5194/bg-12-5967-2015

Novick, K. A., Ficklin, D. L., Stoy, P. C., Williams, C. A., Bohrer, G., Oishi, A. C., … Phillips, R. P. (2016). The increasing importance of atmospheric demand for ecosystem water and carbon fluxes. *Nature Climate Change*, *6*(11), 1023–1027. https://doi.org/10.1038/nclimate3114

Novick, K. A., Stoy, P. C., Katul, G. G., Ellsworth, D. S., Siqueira, M. B. S., Juang, J., & Oren, R. (2004). Carbon dioxide and water vapor exchange in a warm temperate grassland. *Oecologia*, *138*(2), 259–274. https://doi.org/10.1007/s00442-003-1388-z

Oliphant, A. J., & Stoy, P. C. (2018). An evaluation of semiempirical models for partitioning photosynthetically active radiation into diffuse and direct beam components. *Journal of Geophysical Research: Biogeosciences*, *123*(3), 889–901. https://doi.org/10.1002/2017JG004370

Oren, R., Sperry, J. S., Katul, G. G., Pataki, D. E., Ewers, B. E., Phillips, N., & Schäfer, K. V. R. (1999). Survey and synthesis of intra- and interspecific variation in stomatal sensitivity to vapour pressure deficit. *Plant, Cell & Environment*, *22*(12), 1515–1526. https://doi.org/10.1046/j.1365-3040.1999.00513.x

Pau, S., Detto, M., Kim, Y., & Still, C. J. (2018). Tropical forest temperature thresholds for gross primary productivity. *Ecosphere*, *9*(7), e02311. https://doi.org/10.1002/ecs2.2311

Pezeshki, S. R. (1993). Differences in patterns of photosynthetic responses to hypoxia in flood-tolerant and flood-sensitive tree species. *Photosynthetica (Praha)*, *28*(3), 423–430.

Placella, S. A., Brodie, E. L., & Firestone, M. K. (2012). Rainfall-induced carbon dioxide pulses result from sequential resuscitation of phylogenetically clustered microbial groups. *Proceedings of the National Academy of Sciences of the United States of America*, *109*(27), 10931–10936. https://doi.org/10.1073/pnas.1204306109

Reichstein, M., Moffat, A. M., Wutzler, T., & Sickel, K. (2014). REddyProc: Data processing and plotting utilities of (half-) hourly eddy-covariance measurements. *R package version 0.6–0/r9*.

Reichstein, M., Stoy, P. C., Desai, A. R., Lasslop, G., & Richardson, A. D. (2012). Partitioning of net fluxes. In M. Aubinet, T. Vesala, & D. Papale (Eds.), *Eddy covariance* (pp. 263–289). Springer. https://doi.org/10.1007/978-94-007-2351-1_9

Richardson, A. D., Hollinger, D. Y., Burba, G. G., Davis, K. J., Flanagan, L. B., Katul, G. G., … Wofsy, S. C. (2006). A multi-site analysis of random error in tower-based measurements of carbon and energy fluxes. *Agricultural and Forest Meteorology*, *136*(1–2), 1–18. https://doi.org/10.1016/j.agrformet.2006.01.007

Rosseel, Y. (2012). Lavaan: An R package for structural equation modeling and more. Version 0.5–12 (BETA). *Journal of Statistical Software*, *48*(2), 1–36. https://doi.org/10.18637/jss.v048.i02

Saleska, S. R., Miller, S. D., Matross, D. M., Goulden, M. L., Wofsy, S. C., Da Rocha, H. R., … Hutyra, L. (2003). Carbon in Amazon forests: Unexpected seasonal fluxes and disturbance-induced losses. *Science*, *302*(5650), 1554–1557. https://doi.org/10.1126/science.1091165

Santos, D. M., Acevedo, O. C., Chamecki, M., Fuentes, J. D., Gerken, T., & Stoy, P. C. (2016). Temporal scales of the nocturnal flow within and above a forest canopy in Amazonia. *Boundary-Layer Meteorology*, *161*(1), 73–98. https://doi.org/10.1007/s10546-016-0158-5

Schreiber, J. B., Nora, A., Stage, F. K., Barlow, E. A., & King, J. (2006). Reporting structural equation modeling and confirmatory factor analysis results: A review. *The Journal of Educational Research*, *99*(6), 323–338. https://doi.org/10.3200/JOER.99.6.323-338

Spitters, C. J. T., Toussaint, H. A. J. M., & Goudriaan, J. (1986). Separating the diffuse and direct component of global radiation and its implications for modeling canopy photosynthesis Part I. Components of incoming radiation. *Agricultural and Forest Meteorology*, *38*(1–3), 217–229. https://doi.org/10.1016/0168-1923(86)90060-2

Stoy, P. C., Katul, G. G., Siqueira, M. B., Juang, J. Y., Novick, K. A., Uebelherr, J. M., & Oren, R. (2006). An evaluation of models for partitioning eddy covariance-measured net ecosystem exchange into photosynthesis and respiration. *Agricultural and Forest Meteorology*, *141*(1), 2–18. https://doi.org/10.1016/j.agrformet.2006.09.001

Sullivan, M. J. P., Lewis, S. L., Affum-Baffoe, K., Castilho, C., Costa, F., Sanchez, A. C., … Phillips, O. L. (2020). Long-term thermal sensitivity of Earth's tropical forests. *Science*, *368*(6493), 869–874. https://doi.org/10.1126/science.aaw7578

Sulman, B. N., Roman, D. T., Yi, K., Wang, L., Phillips, R. P., & Novick, K. A. (2016). High atmospheric demand for water can limit forest carbon uptake and transpiration as severely as dry soil. *Geophysical Research Letters*, *43*(18), 9686–9695. https://doi.org/10.1002/2016GL069416

Sundari, S., Hirano, T., Yamada, H., Kusin, K., & Limin, S. (2012). Effect of groundwater level on soil respiration in tropical peat swamp forests. *Journal of Agricultural Meteorology*, *68*(2), 121–134. https://doi.org/10.2480/agrmet.68.2.6

Suzuki, S., Ishida, T., Nagano, T., & Waijaroen, S. (1999). Influences of deforestation on carbon balance in a natural tropical peat swamp forest in Thailand. *Environment Control in Biology*, *37*(2), 115–128. https://doi.org/10.2525/ecb1963.37.115

Tang, A. C. I., Stoy, P. C., Hirata, R., Musin, K. K., Aeries, E. B., Wenceslaus, J., & Melling, L. (2018). Eddy covariance measurements of methane flux at a tropical peat forest in Sarawak, Malaysian Borneo. *Geophysical Research Letters*, *45*(9), 4390–4399. https://doi.org/10.1029/2017GL076457

Tang, A. C. I., Stoy, P. C., Hirata, R., Musin, K. K., Aeries, E. B., Wenceslaus, J., … Melling, L. (2019). The exchange of water and energy between a tropical peat forest and the atmosphere: Seasonal trends and comparison against other tropical rainforests. *Science of the Total Environment*, *683*, 166–174. https://doi.org/10.1016/j.scitotenv.2019.05.217

Ueyama, M., Hirata, R., Mano, M., Hamotani, K., Harazono, Y., Hirano, T., … Takahashi, Y. (2012). Influences of various calculation options on heat, water and carbon fluxes determined by open-and closed-path eddy covariance methods. *Tellus B: Chemical and Physical Meteorology*, *64*(1), 19048. https://doi.org/10.3402/tellusb.v64i0.19048

Vick, E. S., Stoy, P. C., Tang, A. C. I., & Gerken, T. (2016). The surface-atmosphere exchange of carbon dioxide, water, and sensible heat across a dryland wheat-fallow rotation. *Agriculture, Ecosystems & Environment*, *232*, 129–140. https://doi.org/10.1016/j.agee.2016.07.018

Vourlitis, G. L., Priante Filho, N., Hayashi, M. M., Nogueira, J. D. S., Caseiro, F. T., &Holanda Campelo Jr., J. (2001). Seasonal variations in the net ecosystem CO_2 exchange of a mature Amazonian transitional tropical forest (cerradao). *Functional Ecology*, *15*(3), 388–395. https://doi.org/10.1046/j.1365-2435.2001.00535.x

Wargan, K., Labow, G., Frith, S., Pawson, S., Livesey, N., & Partyka, G. (2017). Evaluation of the ozone fields in NASA's MERRA-2 reanalysis. *Journal of Climate*, *30*(8), 2961–2988. https://doi.org/10.1175/JCLI-D-16-0699.1

Webb, E. K., Pearman, G. I., & Leuning, R. (1980). Correction of flux measurements for density effects due to heat and water vapour transfer. *Quarterly Journal of the Royal Meteorological Society*, *106*(447), 85–100. https://doi.org/10.1002/qj.49710644707

Wilczak, J. M., Oncley, S. P., & Stage, S. A. (2001). Sonic anemometer tilt correction algorithms. *Boundary-Layer Meteorology*, *99*(1), 127–150. https://doi.org/10.1023/A:1018966204465

Wong, G. X., Hirata, R., Hirano, T., Kiew, F., Aeries, E. B., Musin, K. K., … Melling, L. (2018). Micrometeorological measurement of methane flux above a tropical peat swamp forest. *Agricultural and Forest Meteorology*, *256*, 353–361. https://doi.org/10.1016/j.agrformet.2018.03.025

Wu, J., Guan, K., Hayek, M., Restrepo-Coupe, N., Wiedemann, K. T., Xu, X., … Saleska, S. R. (2017). Partitioning controls on Amazon forest photosynthesis between environmental and biotic factors at hourly to interannual timescales. *Global Change Biology*, *23*(3), 1240–1257. https://doi.org/10.1111/gcb.13509

Xu, J., Morris, P. J., Liu, J., & Holden, J. (2018). PEATMAP: Refining estimates of global peatland distribution based on a meta-analysis. *Catena*, *160*, 134–140. https://doi.org/10.1016/j.catena.2017.09.010

Yulianti, N., & Hayasaka, H. (2013). Recent active fires under El Niño conditions in Kalimantan, Indonesia. *American Journal of Plant Sciences*, *4*(3A), 685–696. https://doi.org/10.4236/ajps.2013.43A087

SUPPORTING INFORMATION

Additional supporting information may be found online in the Supporting Information section.

How to cite this article: Tang ACI, Melling L, Stoy PC, et al. A Bornean peat swamp forest is a net source of carbon dioxide to the atmosphere. *Glob Change Biol*. 2020;26:6931–6944. https://doi.org/10.1111/gcb.15332